Combined forced convection and surface radiation between two parallel plates

Fahad G. Al-Amri and Maged A.I. El-Shaarawi
Department of Mechanical Engineering, College of Technology at Dammam, King Fahd University of Petroleum & Minerals, Dhahran, Saudi Arabia

Received 26 May 2008
Revised 1 January 2009, 18 April 2009
Accepted 15 May 2009

Abstract

Purpose – This paper's aim is to investigate the effect of surface radiation on the developing laminar forced convection flow of a transparent gas between two vertical parallel plates. The walls are heated asymmetrically, this enhances the effect of radiation even with the two walls having low values of emissivity.

Design/methodology/approach – Numerical techniques were used to study the effect of the controlling parameters on wall temperatures, fluid temperature profiles, and Nusslet number.

Findings – The values of the radiation number at which surface radiation can engender symmetric heating (and hence maximum average Nusslet number on the heated wall and maximum reduction in the maximum heated wall temperature are achieved) are obtained. Threshold values of the radiation number at which radiation effects can be neglected are obtained.

Research limitations/implications – Boundary-layer flow model is used.

Practical implications – The implications include design of high-temperature gas-cooled heat exchangers, advanced energy conversion devices, advanced types of power plants, and many others.

Originality/value – Though a number of analyses of internal flows including radiation effect have been made, most have been directed at the simplest case of the prescribed uniform (isothermal) temperature boundary condition. The available literature that deals with the problem with prescribed heat flux at the walls is limited to fully developed flow or specifying the convection coefficient a priori. The lack of both theoretical and experimental data concerning combined forced convection and surface radiation developing flows between two parallel and its practical importance motivated the present work.

Keywords Convection, Gases, Flow, Numerical analysis

Paper type Research paper

Nomenclature

A aspect ratio, ℓ/b

b plate spacing, m

B radiosity of the surface, W/m^2

h local heat-transfer coefficient based on area of heated surface $\left[(\pm k_f \partial T/\partial y|_w)/(T_w - T_m)\right]$, $W/m^2 \cdot K$

$\bar{h}$ average heat-transfer coefficient over the channel height based on average temperature of heated wall $[(Q/\ell(T_{wm} - T_\infty)) = (q/T_{wm} - T_\infty)]$, $W/m^2 \cdot K$

H irradiation, W/m^2

K_f thermal conductivity of fluid, $W/m^2 \cdot K$

ℓ plate length, m

L dimensionless plate length, = A/Re

m number of vertical increments

n number of horizontal increments

N_{rad} radiation number, $\sigma q_1^3 b^4/k_f^4$

Nu_1 local Nusselt number based on area of surface 1 $[(h_1 b/k_f) = (\partial\theta/\partial Y|_{w_1})/(\theta_{w_1} - \theta_m)]$

Nu_2 local Nusselt number based on area of surface 2 $[(h_2 b/k_f) = (\partial\theta/\partial Y|_{w_2})/(\theta_{w_2} - \theta_m)]$

$\bar{N}u_1$ average Nusselt number on wall 1 $\left[(\bar{h}_1 b/k_f) = (Pr\ Re/A) \times [(\theta_m - \theta_\infty)/(\theta_{wm_1} - \theta_\infty)]\right]$

International Journal of Numerical Methods for Heat & Fluid Flow
Vol. 20 No. 2, 2010
pp. 218-239

0961-5539
DOI 10.1108/09615531011016975

$\bar{N}u_2$ average Nusselt number on wall 2 $[(\bar{h}_2\, b/k_f) = (Pr\, Re/A) \times [(\theta_m - \theta_\infty)/(\theta_{wm_2} - \theta_\infty)]]$

p pressure of fluid at any cross section, N/m^2

p' pressure defect at any cross section $[= p + \rho_0 gz]$, N/m^2

p_0 pressure of fluid at channel entrance, N/m^2

P dimensionless pressure at any cross section, $(p' - p_0)/(\rho_0 u_0^2)$

q_j'' heat flux at surface 1 or 2, W/m^2

Q dimensionless heat flux at surface, q_j''/q_1'' [$Q = 1$ at surface 1 and r_H at surface 2]

Q_a rate of heat absorbed by fluid from entrance up to the channel exit, $= [\rho_0\, C_p\, f(T_m - T_\infty)]$, W

r_H heat flux ratio, q_2/q_1

Re Reynolds number, $= (u_o b)/\upsilon$

T temperature at any point, K

T_m mixing-cup temperature over any cross section $\left[= \left(\int_0^b uT\, dy\right) / \int_0^b u\, dy\right]$, K

T_{wm} average temperature of heated wall $\left[= 1/\ell \int_0^\ell T_w\, dZ\right]$, K

T_∞ ambient temperature, K

t thickness of the wall, m

u_o entrance axial velocity, m/s

u longitudinal velocity component at any point, m/s

U dimensionless longitudinal velocity, $U = u/u_o$

v transverse velocity component at any point, m/s

V dimensionless transverse velocity, $V = bv/\upsilon$

y horizontal coordinate, m

Y dimensionless horizontal coordinate, y/b

z vertical coordinate, m

Z dimensionless vertical coordinate, z/(b Re)

Greek symbols

υ kinematic fluid viscosity

ρ fluid density, kg/m^3

μ dynamic fluid viscosity, $kg/m \cdot s$

α thermal diffusivity, m^2/s

β coefficient of thermal expansion, $-1/\rho(\partial\rho/\partial T)_P$, K^{-1}

θ dimensionless temperature at any point $[= k_f T/q_1 b]$

θ_f dimensionless temperature at any point $[= (T - T_m)/(T_{w_1} - T_m)]$

θ_m dimensionless mixing-cup temperature over any cross section $\left[= k_f T_m/q_1 b = \int_0^1 U\theta\, dY / \int_0^1 U\, dY\right]$

θ_{wm} dimensionless average temperature of heated wall $\left[= k_f T_{wm}/q_1 b = 1/L \int_0^L \theta_w\, dZ\right]$

ε wall emissivity

σ Stefan Boltzman constant $= 5.67*10^{-8}$ W/m^2 k^4

Subscripts

e exit

f fluid

i inlet

w wall

1 surface one corresponding to q_1

o ambient or inlet

2 surface two corresponding to q_2

Superscript

′ differential element on the opposing wall

Introduction

The interaction of forced convection and surface radiation at high temperatures and high heat fluxes is important in many technological applications which require high performance and efficiency. These applications include the design of high-temperature gas-cooled nuclear reactors, advanced energy conversion devices, advanced types of power plants, and many others. Though a number of analyses of internal flows including radiation effect have been made, most have been directed at the simplest case of the prescribed uniform (isothermal) temperature boundary condition, which is sometimes inconsistent with reality. The available literature that deals with the problem with prescribed heat flux at the walls is limited to fully developed flow or specifying the convection coefficient a priori. However, these studies showed that the surface radiation can significantly alter the non-radiation results.

Keshock and Siegel (1964) investigated the interaction of surface radiation and convection for a parallel plate channel of finite length with one wall heated and the other adiabatic. Liu and Thorsen (1970) presented a general formulation for determining the gas and wall temperature distribution for both laminar and turbulent flows in parallel plate channels of finite length. They assumed that the velocity profile is known and it was found that for selected values of parameters the local heat-transfer coefficient can actually become negative as the channel exit is approached. Perlmutter and Siegel (1962), Siegel and Perlmutter (1962), and Marcelo (1985) studied the combined forced convection and surface radiation in a tube. The mean fluid velocity and the convective heat-transfer coefficient were assumed constant. Chen (1966), Sikka and Iqbal (1970), Ghoshdastider and Bandyopadhyay (1988), and Razzaque *et al.* (1982) investigated the heat transfer of the hydrodynamically fully developed laminar flow in a circular tube under the radiant heat flux boundary conditions. Gururaja *et al.* (2002) presented a numerical analysis of the problem of two-dimensional, steady, incompressible, conjugate, laminar, mixed convection with surface radiation in a vertical parallel-plate channel, provided with a flush-mounted, heat generating, discrete heat source in each wall. Correlations were evolved for the maximum temperature of the channel walls and the mean friction coefficient. However, his investigation is limited to one discrete heat source in each wall with heat source height equal to 12.5 percent of the total height of the channel. Cadafaleh *et al.* (2003) obtained numerically a correlation for free convection heat transfer in large air channels bounded by one isothermal plate and one adiabatic plate. Surface radiation between plates and different inclination angles are considered. Krishnan *et al.* (2004a, b) presented the results of an experimental and semi-experimental investigation of steady laminar natural convection and surface radiation between three parallel vertical plates, namely, a central hot plate coated with blackboard paint and two unheated side plates that were polished, symmetrically spaced on each side, with air as the inventing medium. The analysis brought out the significance of radiation heat-transfer rate even at low temperature of 310 K. The same authors (Krishnan *et al.*, 2004a, b) gave, based on the measurements, a correlation for the maximum temperature excess of the hot plate in terms of the emissivity of the central and the side plates, the aspect ratio, and the dimensionless total heat flux.

A careful review of the literature failed to disclose any prior work on the effect of surface radiation on the hydro-dynamically and thermally developing flow with non-isothermal boundary conditions between two parallel plates. The lack of both theoretical and experimental data concerning this problem and its practical importance motivated the present work. The present study focuses on the interaction of surface

radiation with forced convection for laminar flow of a transparent gas between two parallel plates.

Convection field equations

Assume steady, laminar, boundary-layer flow of a Newtonian fluid between two vertical parallel plates of constant cross-sectional area as shown in Figure 1. Neglecting viscous dissipation, mass diffusion, chemical reaction, change of phase and electromagnetic effects, the dimensionless equations which govern the laminar forced flow and the heat transfer in the entry-region of vertical parallel plates are:

$$\frac{\partial V}{\partial Y} + \frac{\partial U}{\partial Z} = 0 \tag{1}$$

$$V\frac{\partial U}{\partial Y} + U\frac{\partial U}{\partial Z} = \frac{dP}{dZ} + \frac{\partial^2 U}{\partial Y^2} \tag{2}$$

$$V\frac{\partial \theta}{\partial Y} + U\frac{\partial \theta}{\partial Z} = \frac{1}{Pr}\frac{\partial^2 \theta}{\partial Y^2} \tag{3}$$

The integral form of the continuity Equation (1) is:

$$F = \int_0^1 U\, dY = 1 \tag{4}$$

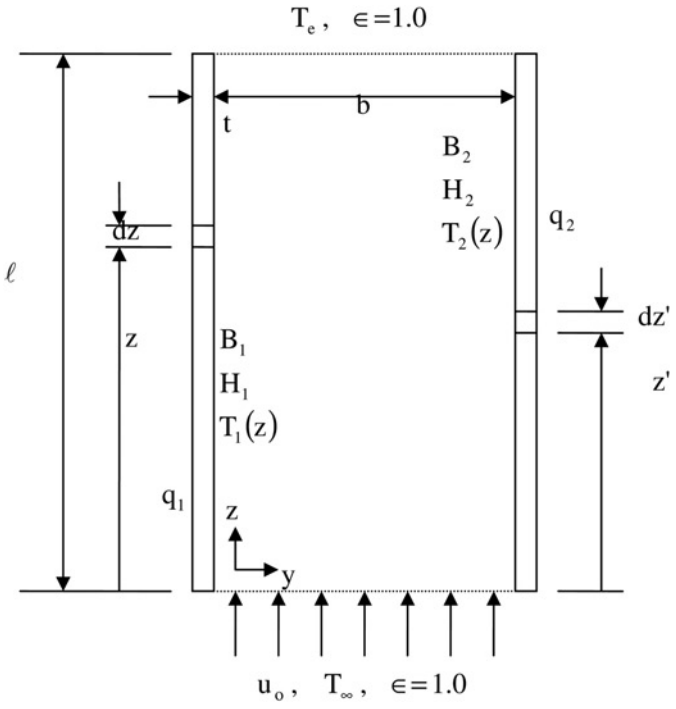

Figure 1.
Schematic of the problem geometry

The dimensionless parameters appearing in Equations (1) to (4) are defined as:

$$Y = \frac{y}{b} \quad Z = \frac{z}{bRe} \quad V = \frac{bv}{\upsilon} \quad U = \frac{u}{\bar{u}} \quad P = \frac{P' - P_O}{\rho_O \bar{u}^2} \quad \theta = \frac{kT}{q_1 b}$$

$$Re = \frac{u\bar{D}}{\upsilon}$$

Boundary conditions

The boundary conditions for the above convection field equations can be written in dimensionless forms as follows:

$$\text{For } Z = 0 \quad \text{and} \quad 0 < Y < 1: \quad U = 1,\ V = P = 0,\ \text{and } \theta = \theta_\infty \tag{5}$$

$$\text{For } Z > 0 \quad \text{and} \quad Y = 0: \quad U = V = 0,\ \text{and } Q = 1 \tag{6}$$

$$\text{For } Z > 0 \quad \text{and} \quad Y = 1: \quad U = V = 0,\ \text{and } Q = r_H \tag{7}$$

Radiation constraint equations

The equation for temperature distribution along each of the two channel walls is derived based on an energy balance. Taking an energy balance on a differential control element at z (see Figure 2), the first law of thermodynamics per unit area of the surface leads to:

$$k_{wj} t \left.\frac{d^2T(z)}{dz^2}\right|_j + q_j(z) + H_j(z) = B_j(z) \pm k_f \left.\frac{\partial T}{\partial y}\right|_j, \quad j = 1, 2 \tag{8}$$

Where $j = 1$ represents the LHS plate, $j = 2$ represents the RHS plate, H(z) and B(z) represent the local irradiation and radiosity of the surfaces at position z and the (+) and (−) signs are for $j = 1$ and $j = 2$, respectively.

However, it was shown by Liu and Thorsen (1970) that the wall conduction term in the above constraint equations does not "qualitatively" influence the interaction between the convection and surface radiation processes. For practical wall thicknesses and wall thermal conductivities, the axial wall conduction has only a small effect on the

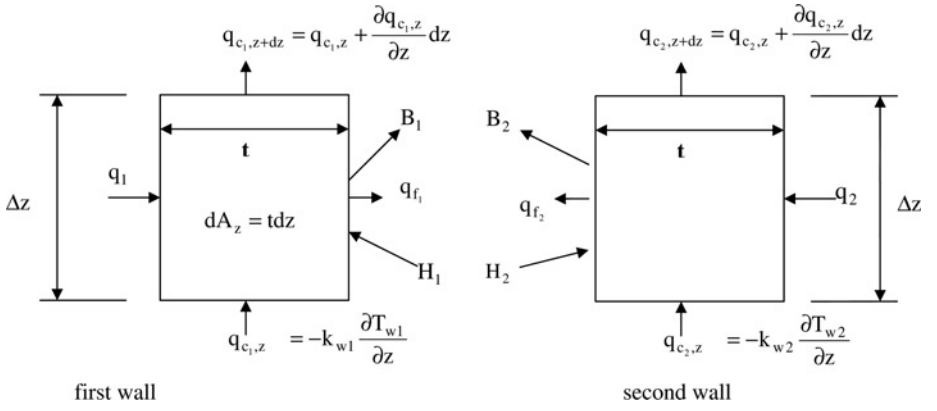

Figure 2.
Control volume for an energy flow

quantitative value of the wall temperature distribution. This result has also been confirmed by results of the present study. Therefore, for the sake of brevity, the effect of axial wall conduction will be neglected. Moreover, in the present study, the inlet and exit channel areas are assumed to be black at the ambient temperature (T_∞) and exit bulk temperature (T_e), respectively. All the surfaces are assumed to be gray, opaque, and diffuse. The shape factors needed to find the irradiation at each element are obtained using the relations given in Keshock and Siegel (1964).

Thus, the above equation, after neglecting axial wall conduction, the substitution of all the relevant expressions, simplification, and non-dimensionalization, leads to the following radiation constraint equations:

Surface 1

$$\begin{aligned}
&1 + N_{rad}\theta_\infty^4\left[\frac{1}{2} - \left(\frac{ZRe}{2}\right)(1 + Z^2Re^2)^{-1/2}\right] \\
&+ N_{rad}\theta_e^4\left[\frac{1}{2} - \left(\frac{(L-Z)Re}{2}\right)(1 + (L-Z)^2\,Re^2)^{-1/2}\right] \\
&+ \int_0^L \left\{\frac{1-\in_2}{\in_2}\left(\left.\frac{\partial\theta}{\partial Y}\right|_{Y=1} - r_H\right) + N_{rad}\theta_{w2}^4(Z)\right\} \\
&* \frac{1}{2}[1 + Re^2(Z-Z')^2]^{(-3/2)}Re\;dZ' = \frac{1-\in_1}{\in_1}\left[-\left.\frac{\partial\theta}{\partial Y}\right|_{Y=0} - 1\right] \\
&+ N_{rad}\;\theta_{w_1}^4(Z) - \left.\frac{\partial\theta}{\partial Y}\right|_{Y=0}
\end{aligned} \tag{9}$$

Where: $N_{rad} = \sigma q_1^3 b^4/k^4$ and $r_H = q_2/q_1$:

Surface 2

$$\begin{aligned}
&r_H + N_{rad}\theta_\infty^4\left[\frac{1}{2} - \left(\frac{ZRe}{2}\right)(1 + Z^2Re^2)^{-1/2}\right] \\
&+ N_{rad}\theta_e^4\left[\frac{1}{2} - \left(\frac{(L-Z)}{2}Re\right)(1 + (L-Z)^2\,Re^2)^{-1/2}\right] \\
&+ \int_0^L \left\{\frac{1-\in_1}{\in_1}\left(-\left.\frac{\partial\theta}{\partial Y}\right|_{Y=0} - 1\right) + N_{rad}\theta_{w1}^4(Z)\right\} \\
&* \frac{1}{2}[1 + Re^2(Z-Z')^2]^{-3/2}\,Re\;dZ' = \frac{1-\in_2}{\in_2}\left[\left.\frac{\partial\theta}{\partial Y}\right|_{Y=1} - r_H\right] \\
&+ N_{rad}\theta_{w_2}^4(Z) + \left.\frac{\partial\theta}{\partial Y}\right|_{Y=1}
\end{aligned} \tag{10}$$

Method of solution

The combined radiation-convection problem is solved based on the following technique. After selecting values of A, P_r, θ_∞, N_{rad}, ε_1 and ε_2, the pure convection field Equations (1) through (3) under the constraint of the integral continuity Equation (4)

and subject to the boundary conditions (5)-(7) are solved using a finite-difference numerical marching technique, the details of which can be found in Coney and El-Shaarawi (1975). On the other hand, the radiation constraint Equations (9) through (10) are solved iteratively using a Gauss-Seidel scheme.

Thus, the solution is broken down into two sub problems. The first involves treating the convection field equations (continuity, momentum, and energy) as an initial value problem and a numerical marching technique is used to obtain a solution. The second involves the solution of Equations (9) and (10) iteratively to update the wall temperatures. These updated wall temperatures will again be used to resolve the convection energy equation. Then, the process is repeated until convergence is achieved. The first iteration assumes no radiation; the radiation constraint equations are replaced by a uniform wall heat flux (UHF), which is equivalent to specifying the temperature gradient. Then, the obtained wall temperatures and temperature gradient are used in the integrals of the radiation constraint Equations (9) and (10) and these two equations are iteratively solved by means of Gauss-Seidel technique.

The results obtained through the solution of Equations (9) and (10) are then used to resolve Equations (1) through (4). The procedure is repeated until the difference between old and new values of temperatures is less than a prescribed tolerance (10^{-6} percent in the present investigation).

Grid independence test

It is well known that the numerical inaccuracy, in any numerical scheme, that results from the truncation errors can be reduced via mesh refinement. As the number of the grid points increases, the accuracy of the solution increases until reach a stage that the accuracy is independent of the grid size. The effect of grid size, i.e. the number of the grid points (m*n), on the present problem is studied as shown in Table I. The grid independence is tested in two stages: (1) m is fixed and n is varied and (2) n is fixed and m is varied. The results of the first stage (with m fixed) indicate that the difference in $\overline{Nu}_1$ between the grid size 1,000*60 and 1,000*100 is 0.0456. The results of the second stage (with n fixed) show that the difference in $\overline{Nu}_1$ between the grid size 1,000*60 and 2,000*60 is 0.1209. Accordingly, m and n have been fixed as 1,000*60, respectively.

Validation of the method

There is no available published work considering the combined radiation and forced convection in the developing region. Therefore, the present numerical code is validated in the combined radiation-convection regime with the fully-developed forced convection work of Liu and Thorsen (1970). On the other hand, there are hydro-dynamically developing forced-convection results without surface radiation (by Heaton

Stage number	m and n	Grid size m * n	$\overline{Nu}_1$	Percentage difference
(1)	m = 1,000 n varied	1,000 * 20	5.0321	–
		1,000 * 60	5.0458	0.2723
		1,000 * 100	5.0481	0.0456
(2)	n = 60 m varied	5,00 * 60	5.0338	–
		1,000 * 60	5.0458	0.2384
		2,000 * 60	5.0519	0.1209

Notes: Re = 500, A = 100, $\theta_\infty = 1$, $N_{rad} = 10$, $\varepsilon = 0.5$ and $r_H = 0$

Table I.
Effect of grid size on the forced convection problem in parallel plate channels

et al. (1964)). These results are used to validate the present numerical code in the hydrodynamically developing regime at considerably low values of surface emissivities.

Figure 3 shows a comparison between the present results for the temperature on the walls in the fully-developed case and those of Liu and Thorsen (1970) with Re = 1,060, Pr = 0.707, A = 20, $N_{rad} = 7.3*10^4$, $\varepsilon = 0.1$, and $\theta_\infty = 0.014$. The obtained results show excellent agreement with the work of Liu and Thorsen (1970). On the other hand, the code is also validated by a special computer run to find the local Nusselt number for very low value of emissivity, $\varepsilon_1 = \varepsilon_2 = \varepsilon = 10^{-6}$. Table II shows a comparison between the pertinent obtained results and the corresponding pure forced-convection results of Heaton *et al.* (1964). This comparison shows a good agreement with the results of Heaton *et al.* (1964).

Results and discussion

Comparing the pure forced-convection case (Heaton *et al.* (1964)) with the present combined radiation-forced convection, the coupling between surface radiative and forced convective heat transfer introduces six additional dimensionless parameters. These parameters are: the two surface emissivities ($\varepsilon_1, \varepsilon_2$), the radiation number ($N_{rad} = \sigma q_1^3 b^4 / k_f^4$), the dimensionless inlet temperature ($\theta_\infty = k_f T_\infty / q_1 b$), the aspect ratio ($A = \ell / b$), and Reynolds number (Re). These six parameters in addition to the pure forced convection parameters, heat flux ratio ($r_H = q_2/q_1$) and Prandtl number

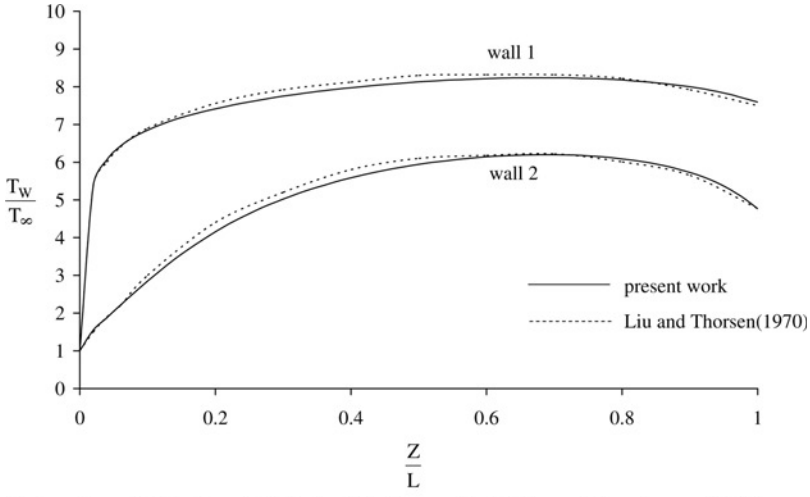

Notes: Re = 1,060, Pr = 0.707, A = 20, $N_{rad} = 7.3*10^4$, $\varepsilon = 0.1$ and $\varepsilon_\infty = 0.014$

Figure 3.
Comparison of walls temperature distribution between the present results of fully developed case and those of Liu and Thorsen (1970)

Z	Nu (Heaton *et al.* (1964))	Nu (present work)	Deviation %
0.0028	9.25	8.41	−9.08
0.0140	4.81	4.55	−5.41
0.0280	3.84	3.74	−2.60
0.1400	2.78	2.78	0
0.2800	2.70	2.70	0
∞	2.70	2.70	0

Table II.
Comparison between present results and those of Heaton *et al.* (1964) for the local Nusselt number between vertical parallel plates

(Pr) are controlling the present problem. With these eight dimensionless parameters, a complete parametric study of the effects of radiation is not feasible. Therefore, the present investigation will be limited to the cases of equal emissivities ($\varepsilon_1 = \varepsilon_2 = \varepsilon$), one wall is heated and the other is adiabatic (i.e. heat flux ratio $r_H = 0$), and a fluid of Pr = 0.707 (air). Thus, the controlling parameters are reduced to only five parameters (ε, N_{rad}, A, θ_∞, and Re).

The main emphasis will be placed on the results that show the effect of the above five controlling parameters on wall temperatures, fluid temperature distribution, and Nusselt number. In addition, threshold values of N_{rad} (the radiation number) at which radiation effect can be neglected will be determined. Finally, radiation numbers at which the combined radiation-convection can produces symmetric heating (even though $r_H = 0$) will be determined.

The ranges chosen for the controlling parameters Re, A, ε, and θ_∞ are:

$$500 \leq \mathrm{Re} \leq 2{,}000$$
$$20 \leq \mathrm{A} \leq 1{,}000$$
$$0 \leq \varepsilon \leq 1$$
$$0.1 \leq \theta_\infty \leq 10$$

The range investigated for the radiation number ($N_{rad} = \sigma q_1^3 b^4/k^4$), and the corresponding ranges for plate spacing (b), and heat input (q_1) are shown in Table III for three selected values of the dimensionless inlet temperature.

The above ranges of dimensionless inlet temperature and radiation number are chosen to have a wide range of heat input for both the close spacing and the large spacing.

To understand the physics of the problem, the wall temperatures and the fluid temperature profiles of are presented first. Due to space limitations, only a sample of the results will be presented here. Unless otherwise stated, the presented sample of results is for the following controlling parameters values: dimensionless inlet temperature (θ_∞) = 3, radiation number (N_{rad}) = 0.03, aspect ratio (A) = 500, emissivity(ε) = 0.9, and Reynolds number (Re) = 1,000.

Effect of surface radiation on wall temperatures and fluid temperature profiles

Figures 4 (a), (b), and (c) show the variation of the wall temperatures and the mixed-mean temperature with the distance from entrance for both the combined radiation-forced convection case and the pure forced-convection case for three selected values of the aspect ratio namely, 50, 100, and 500 respectively. In these figures the wall/fluid temperature is normalized using the dimensionless inlet temperature. The figures show that the surface radiation reduces the temperature of the heated wall and increases the temperature of the unheated wall, when compared with the pure-forced

Table III.
Range investigated for the radiation number ($N_{rad} = \sigma q_1^3 b^4/k^4$)

θ_∞	N_{rad}	b(m)	$q_1(w/m^2)$
0.1	60-3*10^4	0.001-0.5	150.0-8*10^4
1.0	0.06-30	0.001-0.5	15.0-8,000
10.0	0.00006-0.03	0.001-0.5	1.5-800

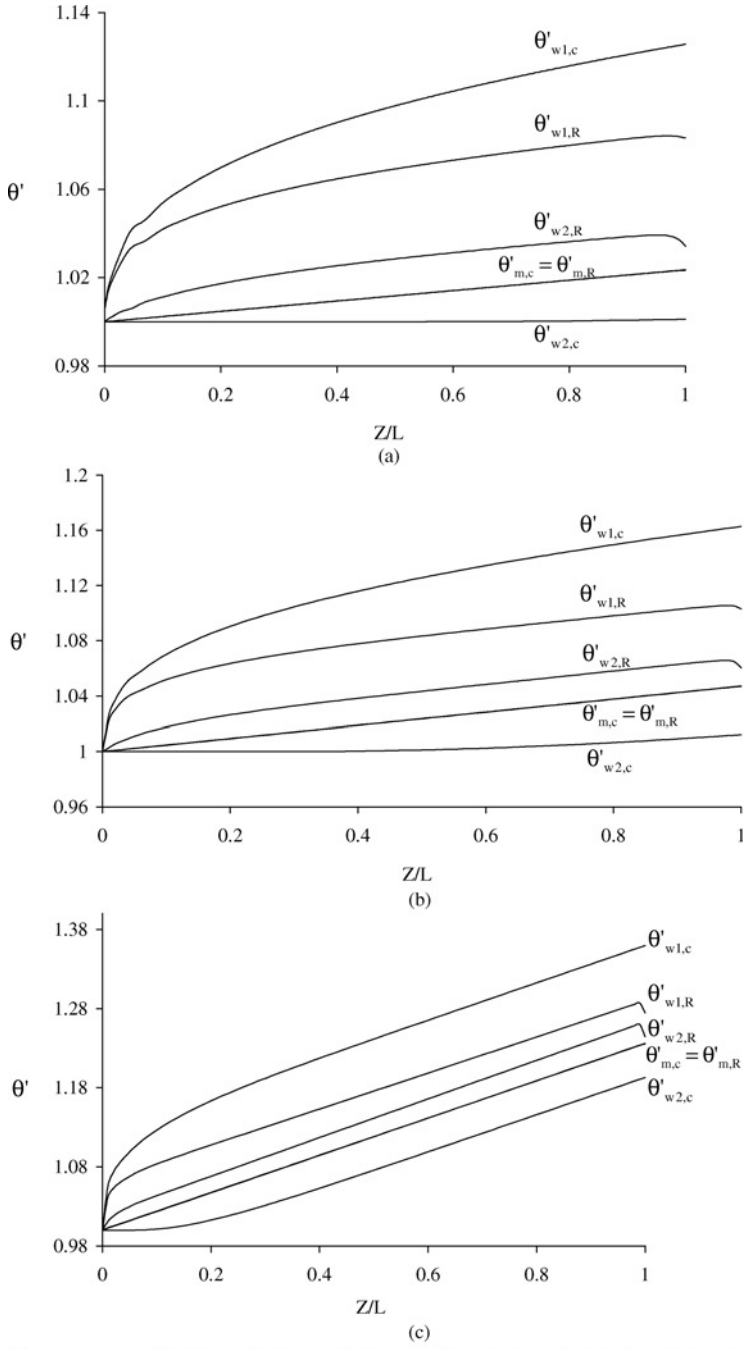

Notes: Re = 1,000, $\theta_\infty = 3$, $N_{rad} = 0.03$, $\varepsilon = 0.9$: (a) A = 50, (b) A = 100 and (c) A = 500

Figure 4.
Walls and mixing-cup temperatures for the combined radiation-convection and the pure convection solutions

convection case. The dip in the wall temperature near the exit is due to the relatively large value of radiation transfer directly to the exit.

The above figures indicate that the combined radiation-convection two wall temperatures can be not at all close to the pure-convection results; they rather lie midway between them. In contrast, the mixing-cup (mixed-mean) temperature, for the parameters chosen ($\theta_\infty = 3$, $N_{rad} = 0.03$, $A = 500$, $\varepsilon = 0.9$, $r_H = 0$, $Re = 1{,}000$, $Pr = 0.707$), are identical in both cases for all the three chosen values of the aspect ratio ($A = 50$, 100, and 500). This is because the heat input to the fluid, as per the imposed boundary conditions, is almost the same in both cases for such a low value of N_{rad}.

Figure 5 shows typical normalized fluid temperature (T/T_∞, i.e. θ/θ_∞) profiles at different longitudinal distances from the entrance, for both the combined radiation-convection and the pure-convection solutions. It is clear from this figure that surface radiation has a noticeable effect on the fluid temperature; surface radiation decreases the fluid temperature near the heated wall and increases it near the unheated wall. In addition, the radiation effect is as if it transfers some of the convective heat flux from the heated wall to the unheated wall and hence reduces the heated-wall temperature gradient while it increases such a gradient on the externally adiabatic wall to make it internally active (i.e. it transfers heat by convection to the moving fluid even though it is externally adiabatic).

Figure 6 (a), (b), and (c) show the effect of radiative heat transfer on local fluid temperature ($\theta_f = (T - T_m)/(T_{w1} - T_m)$) for aspect ratios (A) 50, 100, and 500, respectively. For a short channel ($A = 50$), the portion near the unheated wall ($Y > 0.8$) can become thermally fully developed. In contrast, for long channel ($A = 500$), only the portion near the heated wall ($Y \leq 0.1$) can be thermally fully developed. This means that the thermally fully developed solution cannot be obtained with radiation present (except at a value of the radiation number that can produce symmetric heating as will be shown later).

Effect of surface radiation on local Nusselt number

Figure 7 shows the variation of the local Nusselt number on the uniformly heated wall with the dimensionless distance Z/L for the selected aspect ratios (A) 50, 100, and 500. It is clear from this figure that as the aspect ratio increases the local Nusselt number on the heated side attains its asymptotic value at smaller distance from the entrance

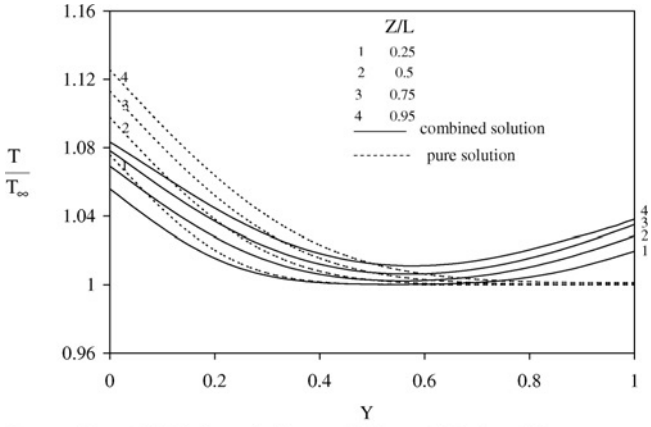

Figure 5.
Cross-channel temperature profiles of air for both combined and pure convection solutions

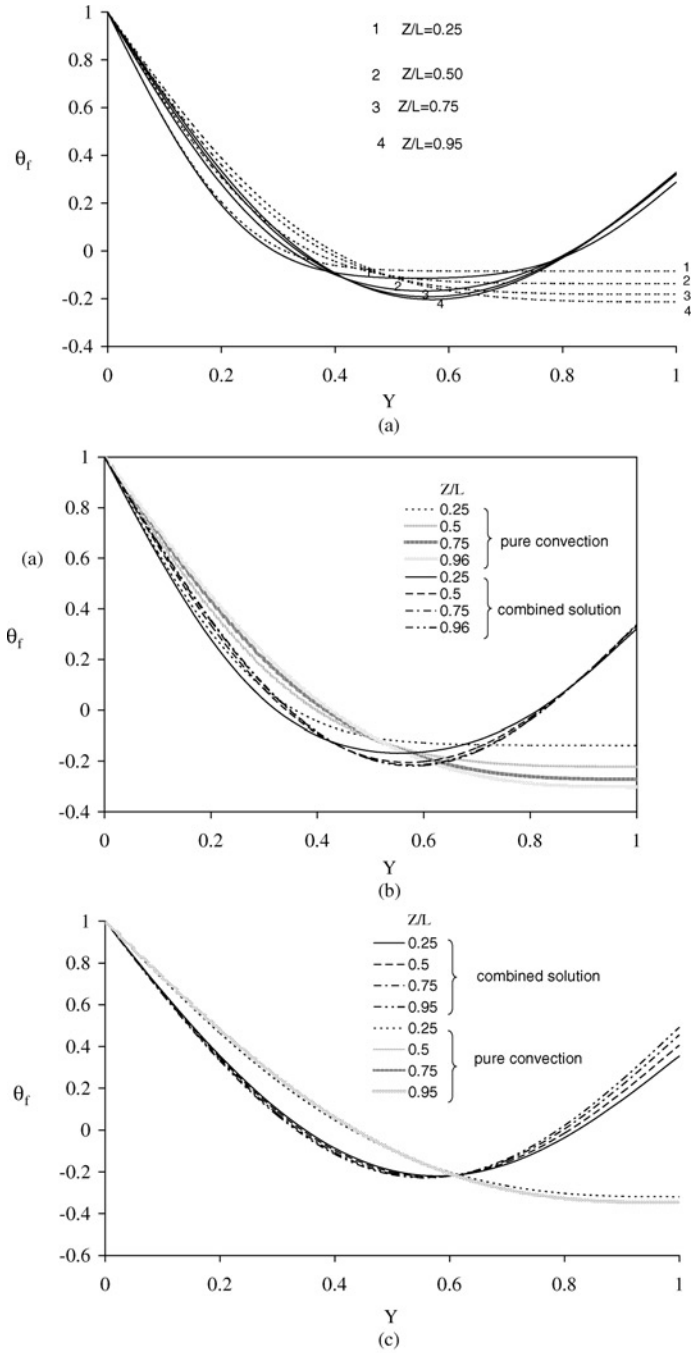

Notes: Re = 1,000, $\theta_\infty = 3$, $N_{rad} = 0.03$, $\varepsilon = 0.9$: (a) A = 50, (b) A = 100 and (c) A = 500

Figure 6.
Cross-channel temperature profiles of air for both combined and pure convection solutions

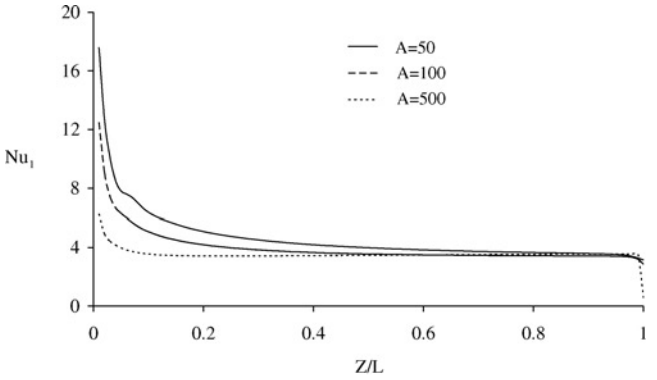

Notes: Re = 1,000, $\theta_\infty = 3$, $N_{rad} = 0.03$ and $\varepsilon = 0.9$

Figure 7.
Local Nusselt number on the heated side

(smaller values of Z/L). This is because, as was shown before, the fluid in the portion of the channel near the heated wall becomes thermally fully developed in such long channel. On the other hand, the externally adiabatic wall is also heating the fluid (it is internally active) as a result of being heated by the heat radiation that it receives from the heated wall. The local Nusselt number on this unheated wall attains its asymptotic value for short channel (low values of A) as shown in Figure 8; this is because the fluid near this wall becomes thermally fully developed. For long channels, the local Nusselt number on the unheated wall continued to decrease and cannot attain an asymptotic value as shown in the figure.

Effect of radiation number

Figure 9 shows the effect of radiation number ($N_{rad} = \sigma q_1^3 b^4 / k_f^4$) on the fluid temperature profiles ($\theta_f = (T - T_m)/(T_{w1} - T_m)$) at $Z = 0.5$. As the radiation number increases the fluid temperature profile becomes closer to symmetry. Increasing the radiation number increases the amount of heat radiated that crosses the gap to the unheated plate until both the externally adiabatic and the heated surface temperatures become the same as clarified in Figure 10.

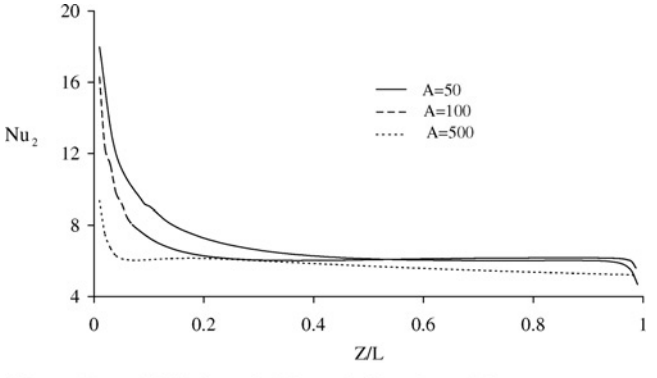

Notes: Re = 1,000, $\theta_\infty = 3$, $N_{rad} = 0.03$ and $\varepsilon = 0.9$

Figure 8.
Local Nusselt number on the unheated side

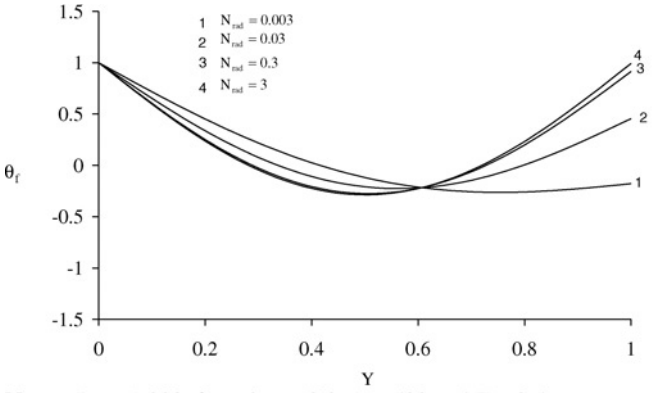

Notes: Re = 1,000, $\theta_\infty = 3$, $\varepsilon = 0.9$, A = 500 and Z = 0.5

Figure 9.
Cross-channel temperature profiles of air for different radiation numbers

Figures 11 and 12 show the effect of the radiation number on the local Nusselt number on the heated wall and on the unheated wall, respectively. The local Nusselt number on the heated wall increases as the radiation number increases. For the chosen radiation numbers, it reaches an asymptotic value when the flow reaches thermal full development as shown in the figure.

At considerably low radiation number, the local Nusselt number on the unheated wall can be negative allover the channel length. This is because the unheated wall is not supplying heat to the fluid, on the contrary it absorbs heat, and the term $(T_{w2} - T_m)$, in the definition of the local Nusselt number, is negative. At entrance $(Z/L = 0)$, the local Nusselt number on the unheated wall is infinite ($-\infty$ for considerably low radiation numbers or $+\infty$ for large values of radiation number). This is because the boundary layer thickness is zero at this particular location and merely, in the definition of the local Nusselt number, $T_{w2} - T_m = 0$. For a given radiation number, the absolute value of the local Nusselt number on the unheated wall decreases until it reaches its asymptotic value when the flow reaches thermal full development as shown in Figure 12. At very high radiation number, the combined radiation-forced

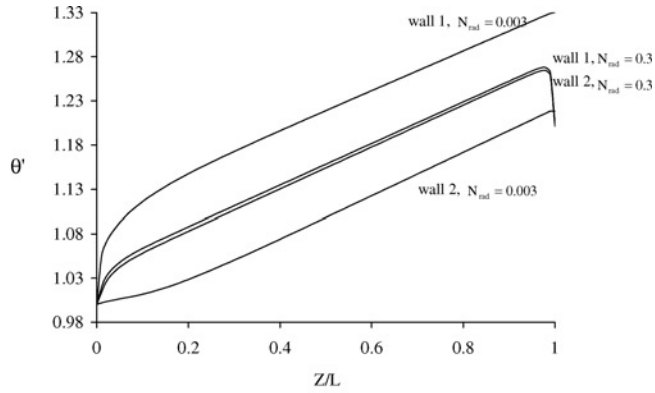

Notes: Re = 1,000, $\theta_\infty = 3$, $\varepsilon = 0.9$ and A = 500

Figure 10.
Walls temperature for different radiation numbers

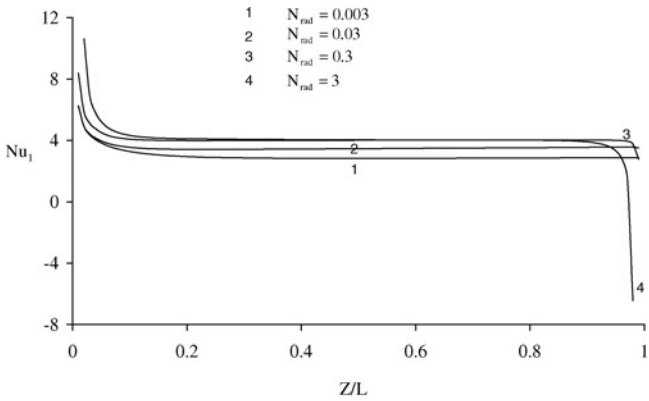

Figure 11.
Local Nusselt number on heated side for different radiation numbers

Notes: Re = 1,000, $\theta_\infty = 3$, $\varepsilon = 0.9$ and A = 500

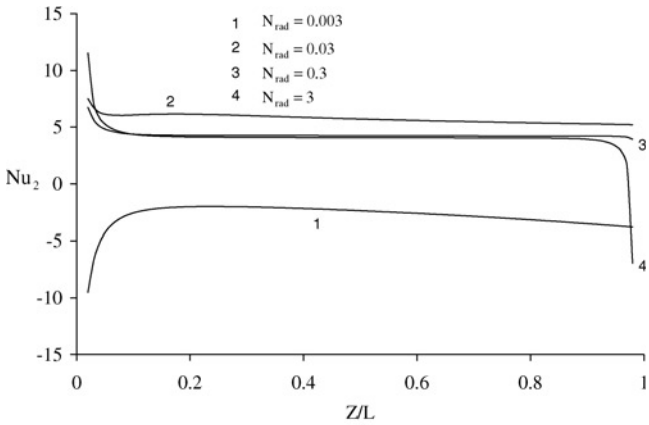

Figure 12.
Local Nusselt number on unheated side for different radiation numbers

Notes: Re = 1,000, $\theta_\infty = 3$, $\varepsilon = 0.9$ and A = 500

convection heat transfer can behave similar to a pure forced convection with symmetric heating as shown in Figures 13 and 14. However, the wall temperatures and the mixing-cup (mixed-mean) temperature of the combined solution in this case are lower than those obtained by pure convection with symmetric heating, as shown in Figure 15. The radiation number at which symmetric heating can occur will hereinafter be referred to as the symmetric radiation number ($N_{r,symm}$).

The effect of the radiation number on the average Nusselt number on the heated wall is shown in Figure 16. It is clear that the average Nusselt number first increases rapidly with the radiation number then it increases gradually and attains an asymptotic value at the symmetric radiation number. The values of the average Nusselt number are always between two limiting values corresponding to two pure convection solutions: one with one wall heated while the other wall is adiabatic ($r_H = 0$) and the second of symmetric heating ($r_H = 1$).

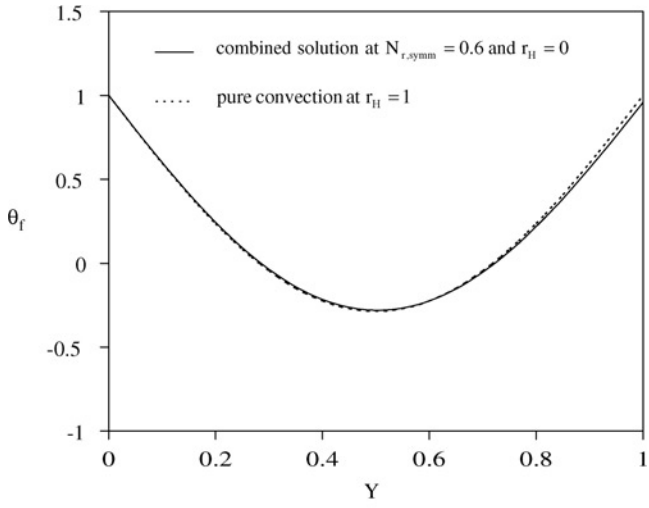

Notes: Re = 1,000, $\theta_\infty = 3$, $\varepsilon = 0.9$ and A = 500

Figure 13.
Cross-channel temperature profiles of air for combined solution at radiation number that causes symmetric heating and the pure convection solution with real symmetric heating

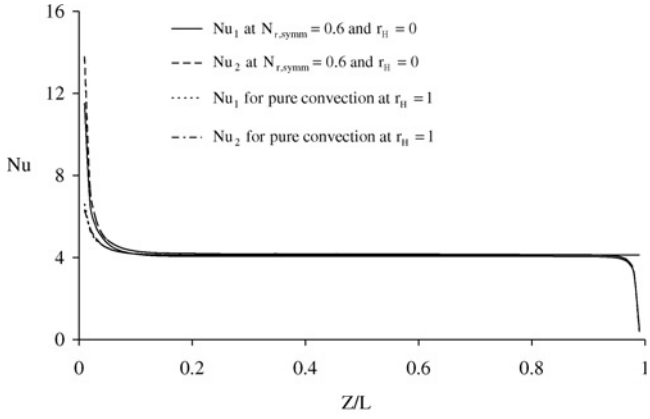

Notes: Re = 1,000, $\theta_\infty = 3$, $\varepsilon = 0.9$ and A = 500

Figure 14.
Local Nusselt numbers for combined solution at radiation number that causes symmetric heating and the pure convection solution with real symmetric heating

Effect of heat flux ratio

Figure 17 shows the percentage of the average radiation heat transfer to the total heat transfer from the heated wall as a function of heat flux ratio, r_H. The figure shows that the radiation transfer linearly decreases as the heat flux increases. The radiation effect is less than 10 percent of the total heat transfer and can be neglected for heat flux ratio $(r_H) \geq 0.8$.

Effect of dimensionless channel length

Figure 18 shows the percentage of average radiation heat transfer to the total heat transfer from the heated wall as a function of the dimensionless channel length, A/Re for three selected values of r_H (including the limiting values of $r_H = 0$ and 1). For

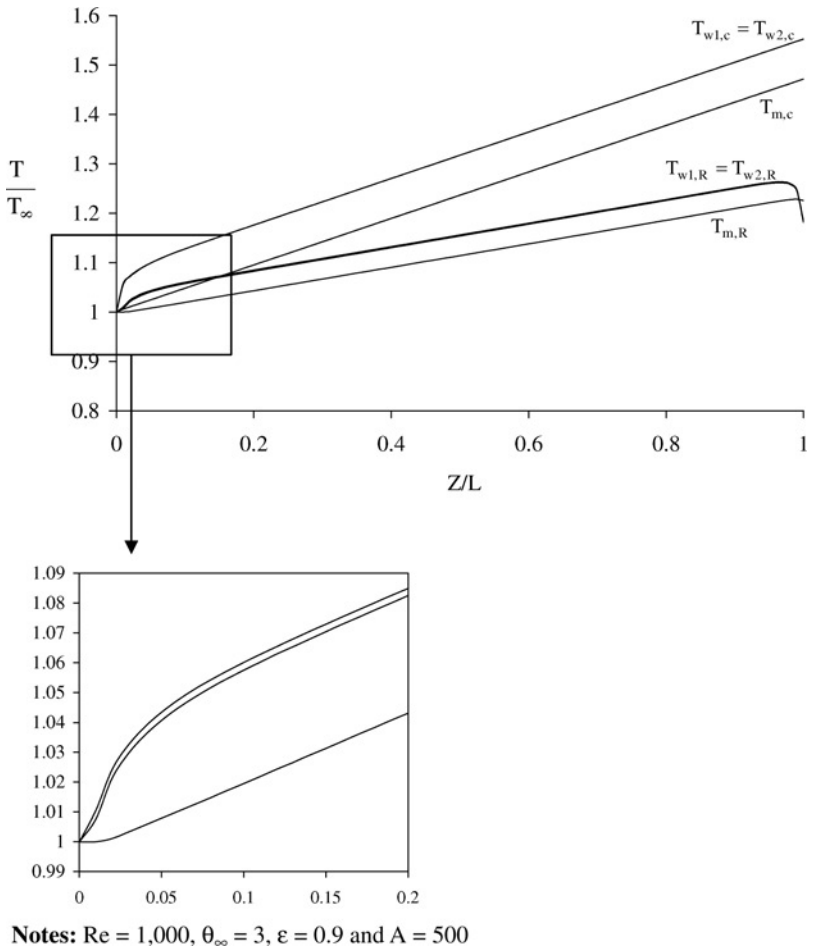

Notes: Re = 1,000, $\theta_\infty = 3$, $\varepsilon = 0.9$ and A = 500

Figure 15.
Wall temperatures and mixing-cup temperatures for combined solution at symmetric radiation number and the pure convection solution with real symmetric heating

symmetric heating ($r_H = 1$), the wall temperature of the two surfaces are the same which negates radiation heat transfer for all values of the dimensionless length; thus the corresponding values of $\overline{Qr}_1$ percent are zero as shown in the figure. For zero heat flux ratio ($r_H = 0$), the radiation transfer increases as the dimensionless length increases. The case of $r_H = 0.2$ has noticeable radiation heat transfer and consequently its results are qualitatively similar to that of $r_H = 0$.

Threshold values of radiation number

The threshold values of the radiation number below which radiation can be neglected for a given dimensionless inlet temperature (θ_∞) are of practical importance. These values are given for three selected values of $\theta_\infty = 0.1$, 1, and 10 in Tables IV-VI, respectively. The threshold values of the radiation number have been arbitrarily defined in the present work as the values at which the percentage of the average radiation transfer to the total heat transfer from the heated wall is 10 percent. The fraction of the radiation heat transfer to the total is the difference between the local heat input per unit area Q = 1 (constant) and the local convective heat flux (assuming the

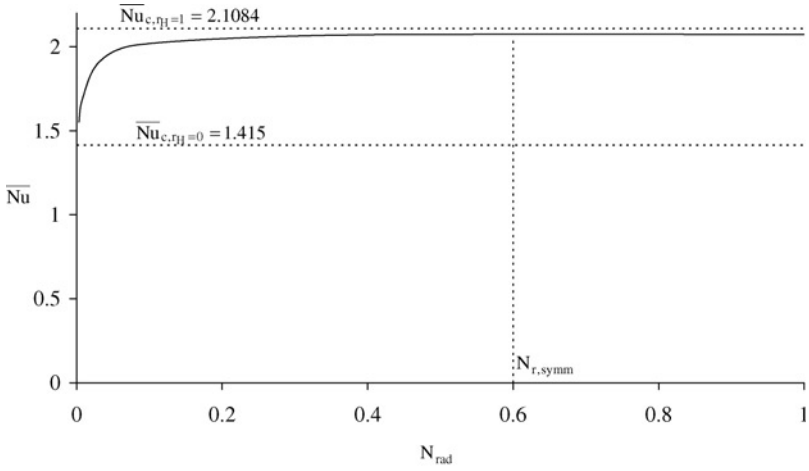

Notes: Re = 1,000, $\theta_\infty = 3$, $\varepsilon = 0.9$ and A = 500

Figure 16.
Average Nusselt number on heated wall as a function of radiation number

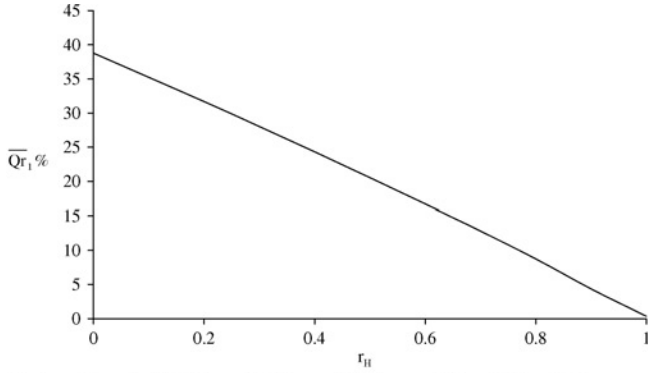

Notes: Re = 1,000, $\theta_\infty = 3$, $N_{rad} = 0.03$, $\varepsilon = 0.9$ and A= 500

Figure 17.
Percentage of average radiation heat transfer on heated wall as a function of heat flux ratio

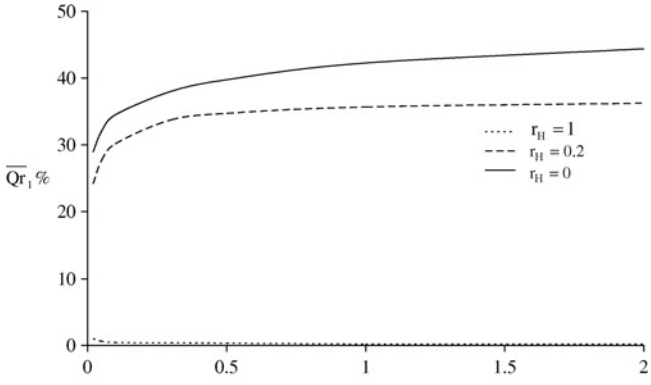

Notes: $\theta_\infty = 3$, $N_{rad} = 0.03$ and $\varepsilon = 0.9$

Figure 18.
Percentage of average radiation heat transfer on heated wall as a function of dimensionless length

axial wall heat conduction is negligible), i.e.,

$$Q_r = \left(1.0 + \left.\frac{\partial\theta}{\partial Y}\right|_{Y=0}\right)$$

The average radiation transfer can be obtained as follows:

$$\overline{Q_r} = \frac{\int_0^L Q_r dZ}{L}$$

These tables show that the radiation effect increases as the dimensionless inlet temperature decreases. It is also found that for inlet temperature (θ_∞) ≤ 0.025 the

	A = 20			A = 200			A = 1,000		
ε	Re = 500	1,000	2,000	Re = 500	1,000	2000	Re = 500	1,000	2,000
0.05	240	480	880	–	–	–	–	–	–
0.25	–	90	190	–	–	–	–	–	–
0.50	–	–	80	–	–	–	–	–	–
0.75	–	–	–	–	–	–	–	–	–
0.95	–	–	–	–	–	–	–	–	–

Table IV.
Threshold values of radiation number

Note: $\theta_\infty = 0.1$

	A = 20			A = 200			A = 1,000		
ε	Re = 500	1,000	2,000	Re = 500	1,000	2,000	Re = 500	1,000	2,000
0.05	2.800	3.600	5.000	0.910	1.300	1.900	0.120	0.370	0.690
0.25	0.500	0.750	0.990	0.150	0.250	0.350	–	0.060	0.130
0.50	0.230	0.340	0.460	0.070	0.100	0.150	–	–	0.060
0.75	0.130	0.180	0.270	–	0.060	0.080	–	–	–
0.95	0.084	0.130	0.180	–	–	–	–	–	–

Table V.
Threshold values of radiation number

Notes: means there is no threshold value, i.e. radiation can not be neglected; radiation is higher than 10 percent of the total heat transfer; $\theta_\infty = 1.0$

	A = 20			A = 200			A = 1,000		
ε	Re = 500	1,000	2,000	Re = 500	1,000	2,000	Re = 500	1,000	2,000
0.05	0.00350	0.00450	0.00550	0.002100	0.00250	0.00300	0.00150	0.00180	0.00220
0.25	0.00074	0.00094	0.00120	0.000400	0.00045	0.00055	0.00027	0.00035	0.00041
0.50	0.00034	0.00043	0.00055	0.000170	0.00020	0.00024	0.00012	0.00015	0.00018
0.75	0.00019	0.00024	0.00033	0.000100	0.00012	0.00014	0.00007	0.00008	0.00010
0.95	0.00012	0.00017	0.00022	0.000065	0.00008	0.00009	–	–	0.00006

Table VI.
Threshold values of radiation number

Note: $\theta_\infty = 10.0$

radiation effect can not be neglected for all values of controlling parameters under consideration in the present investigation.

Values of radiation number to achieve symmetric heating

The values of the radiation number at which symmetric heating can occur for a given dimensionless inlet temperature are shown in Tables VII-IX for the three selected values of A and for $\theta_\infty = 0.1$, 1.0 and10.0, respectively. These values are referred to as the symmetric radiation numbers and they have been arbitrarily defined in the present work as the values at which the average Nusselt number of the combined solution approaches within 5 percent the average Nusselt number of the pure convection with symmetric heating ($r_H = 1$). At these values of radiation number, the maximum value of the average Nusselt number on the uniformly heated wall and the maximum reduction in the maximum wall temperature are achieved.

	A = 20			A = 200			A = 1,000		
ε	Re = 500	1,000	2,000	Re = 500	1,000	2,000	Re = 500	1,000	2,000
0.05	NSO	NSO	NSO	1,300	4,600	8,100	AS	190	500
0.25	7,000	15,000	28,000	380	880	1,800	AS	AS	100
0.50	4,000	4,600	6,000	180	400	900	AS	AS	60
0.75	2,200	3,170	5,000	70	250	570	AS	AS	AS
0.95	1,880	2,570	4,000	AS	100	340	AS	AS	AS

Notes: *NSO: no symmetric heating occurs; **AS: always symmetric; $\theta_\infty = 0.1$

Table VII.
Symmetric values of radiation number

	A = 20			A = 200			A = 1,000		
ε	Re = 500	1,000	2,000	Re = 500	1,000	2,000	Re = 500	1,000	2,000
0.05	NSO*	NSO	NSO	NSO	NSO	NSO	5.00	15.00	30.00
0.25	NSO	NSO	NSO	10	20	40	0.30	1.50	4.00
0.50	NSO	NSO	NSO	3.1	6.7	12.5	0.10	0.59	1.50
0.75	NSO	NSO	NSO	1.7	3.4	6.1	AS**	0.33	0.80
0.95	NSO	NSO	NSO	1.0	2.2	3.8	AS	0.21	0.57

Notes: *NSO: no symmetric heating occurs; **AS: always symmetric; $\theta_\infty = 1.0$

Table VIII.
Symmetric values of radiation number

	A = 20			A = 200			A = 1,000		
ε	Re = 500	1,000	2,000	Re = 500	1,000	2,000	Re = 500	1,000	2,000
0.05	NSO	NSO	NSO	NSO	NSO	NSO	NSO	NSO	NSO
0.25	NSO	NSO	NSO	NSO	NSO	NSO	0.00220	0.00820	0.0140
0.50	NSO	NSO	NSO	NSO	NSO	NSO	0.00085	0.00250	0.00410
0.75	NSO	NSO	NSO	NSO	NSO	NSO	0.00047	0.00130	0.0030
0.95	NSO	NSO	NSO	0.00250	0.00440	0.00860	0.00030	0.00090	0.0020

Notes: *NSO: no symmetric heating occurs; **AS: always symmetric; $\theta_\infty = 10.0$

Table IX.
Symmetric values of radiation number

Conclusion

Surface radiation can drastically affect the forced convection heat-transfer parameters. Even in the extreme case of asymmetric heating with $r_H = 0$, surface radiation can engender symmetric fluid heating. Values of the radiation numbers at which symmetric fluid heating can be achieved have been obtained for selected values of the surface emissivity (ε), the aspect ratio (A), the inlet fluid temperature (θ_∞), and the Reynolds number. Similarly, the radiation numbers at which surface radiation can practically be neglected in the forced convection flow have been obtained.

References

Cadafaleh, J., Oliva, A., Van der Graaif, G. and Albets, X. (2003), "Natural convection in a large, inclined channel with asymmetric heating and surface radiation", *Journal of Heat Transfer*, Vol. 125, pp. 812-20.

Chen, J.C. (1966), "Laminar heat transfer in a tube with nonlinear radiant heat flux boundary condition", *International Journal of Heat Mass Transfer*, Vol. 9 No. 5, pp. 433-40.

Coney, J.E.R. and El-Shaarawi, M.A.I. (1975), "Finite difference analysis for laminar flow heat transfer in concentric annuli with simultaneously developing hydrodynamic and thermal boundary layers", *International Journal for Numerical Methods in Engineering*, Vol. 9, pp. 17-38.

Gururaja Rao, C., Balaji, C. and Venkateshan, S.P. (2002), "Effect of surface radiation on conjugate mixed convection in a vertical channel with a discrete heat source in each wall", *International Journal of Heat and Mass Transfer*, Vol. 45, pp. 3331-47.

Heaton, H.S., Reynolds, W.C. and Kays, W.M. (1964), "Heat transfer in annular passages. Simultaneous development of velocity and temperature fields in laminar flow", *International Journal of Heat Mass Transfer*, Vol. 7, pp. 763-81.

Keshock, E.G. and Siegel, R. (1964), "Combined radiation and convection in a asymmetrically heated plate flow channel", *Journal of Heat Transfer*, Vol. 86 No. 3, pp. 341-50.

Krishnan, A.S., Balaji, C. and Venkateshan, S.P. (2004a), "An experimental correlation for combined convection and radiation between parallel vertical plates", *Journal of Heat Transfer*, Vol. 126, pp. 849-51.

Krishnan, A.S., Premachandran, B., Balaji, C. and Venkateshan, S.P. (2004b), "Combined experimental and numerical approach to multimode heat transfer between vertical parallel-plates", *Experimental Thermal and Fluid Science*, Vol. 29 No. 1, pp. 75-86.

Liu, S.T. and Thorsen, R.S. (1970), "Combined forced convection and radiation heat transfer in asymmetrically heated parallel plates", *Proceedings of the Heat Transfer and Fluid Mechanics Institute*, Stanford University Press, Palo Alto, CA, pp. 32-44.

Marcelo, J.S.L. (1985), "Radiant and convective heat transfer for flow of a transparent gas in a short tube with Sinusoidal Wall Heat Flux", *International Communications on Heat Mass Transfer*, Vol. 12, pp. 505-20.

Perlmutter, M. and Siegel, R. (1962), "Heat transfer by combined forced convection and thermal radiation in a heated tube", *Journal of Heat Transfer*, Vol. 84 No. 4, pp. 301-11.

Razzaque, M.M., Howell, J.R. and Klein, D.E. (1982), "Finite element solution of heat transfer for gas flow through a tube", *AIAA Journal*, Vol. 20 No. 7, pp. 1015-9.

Siegel, R. and Perlmutter, M. (1962), "Convective and radiant heat transfer for flow of a transparent gas in a tube with a Gray Wall", *International Journal of Heat Mass Transfer*, Vol. 5 No. 7, pp. 639-60.

Sikka, S. and Iqbal, M. (1970), "Laminar heat transfer in a circular tube under solar radiation in space", *International Journal of Heat Mass Transfer*, Vol. 13 No. 6, pp. 975-83.

Further reading

Ghoshdastidar, P.S. and Bandyopadhyay, A. (1988), "Conjugate heat transfer in the laminar flow of high Prandtl number fluid in a circular tube subjected to non-uniform circumferential radiation heat flux from a large heated wall", *Proceedings of the 25th National Heat Transfer Conference, Vol. 1, ASME HTD-96, American Society of Mechanical Engineers, New York, NY, July*, pp. 153-61.

Corresponding author

Maged A. I. El-Shaarawi can be contacted at: magedas@kfupm.edu.sa